

OPEN ACCESS

Optimization of Sodium Bis(oxalato)borate (NaBOB) in Triethyl Phosphate (TEP) by Electrolyte Additives

To cite this article: Jonas Welch *et al* 2022 *J. Electrochem. Soc.* **169** 120523

View the [article online](#) for updates and enhancements.

ECS Toyota Young Investigator Fellowship



For young professionals and scholars pursuing research in batteries, fuel cells and hydrogen, and future sustainable technologies.

At least one \$50,000 fellowship is available annually.
More than \$1.4 million awarded since 2015!



Application deadline: January 31, 2023

Learn more. Apply today!



Optimization of Sodium Bis(oxalato)borate (NaBOB) in Triethyl Phosphate (TEP) by Electrolyte Additives

Jonas Welch,¹ Ronnie Mogensen,¹ Wessel van Ekeren,¹ Henrik Eriksson,² Andrew J. Naylor,¹ and Reza Younesi^{1,z} 

¹Department of Chemistry—Ångström Laboratory, Uppsala University, 75121 Uppsala, Sweden

²LiFeSiZE AB, SE-754 50 Uppsala, Sweden

The electrolyte solution of NaBOB in TEP is a low-cost, fluorine-free and flame-retardant electrolyte with ionic conductivity of 5 mS cm⁻¹, recently discovered to show promises for sodium-ion batteries. Here, the abilities of this electrolyte to effectively form a solid electrolyte interphase (SEI) was augmented with five common electrolyte additives of fluoroethylene carbonate (FEC), vinylene carbonate (VC), prop-1-ene-1,3-sultone (PES), 1,3,2-dioxathiolane 2,2-dioxide (DTD) and tris(trimethylsilyl)phosphite (TTSPi). Full-cells with electrodes of Prussian white and hard carbon and industrial mass loadings of >10 mg cm⁻² and electrolyte volumes of <5 ml g⁻¹ were used. X-ray photoelectron spectroscopy (XPS) and pressure analysis were also deployed to investigate parasitic reactions. Cells using electrolyte additives of PES, PES+DTD and PES+TTSPi (3 wt%) showed significantly increased performance in terms of capacity retention and initial Coulombic efficiency as compared to additive-free NaBOB-TEP. The best cell retained 80% discharge capacity (89 mAh g⁻¹) after 450 cycles, which is also significantly better than reference cells using 1 M NaPF₆ in EC:DEC electrolyte. This study sheds light on opportunities to optimize the NaBOB-TEP electrolyte for full-cell sodium-ion batteries in order to move from low-mass-loading lab-scale electrodes to high mass loading electrodes aiming for commercialization of sodium-ion batteries.

© 2022 The Author(s). Published on behalf of The Electrochemical Society by IOP Publishing Limited. This is an open access article distributed under the terms of the Creative Commons Attribution 4.0 License (CC BY, <http://creativecommons.org/licenses/by/4.0/>), which permits unrestricted reuse of the work in any medium, provided the original work is properly cited. [DOI: 10.1149/1945-7111/aca5e]



Manuscript submitted September 9, 2022; revised manuscript received November 22, 2022. Published December 23, 2022.

Supplementary material for this article is available [online](#)

To facilitate the use of renewable energies, further expansion in energy storage in the form of batteries is needed. Today, the use of lithium-ion batteries (LIBs) in different applications is widely adopted. However, LIBs come with some concerns including increased demands on use of non-abundant natural elements used in LIBs, i.e. lithium, cobalt, nickel and copper.¹ Another concern is the use of flammable electrolytes that can ignite and combust, forming poisonous fluorinated compounds such as hydrofluoric acid, HF, due to the use of lithium hexafluorophosphate salt (LiPF₆).² Materials for the high voltage LIBs of today also require very careful manufacture process to avoid moisture, thus the harmful solvent N-Methyl-2-pyrrolidone (NMP), which requires energy intensive solvent recycling, is commonly used for electrode preparation.³ To address aforementioned concerns, sodium-ion batteries (SIBs) in which (i) electrode materials are synthesized from abundant elements and (ii) non-flammable and fluorine-free electrolytes are used, have been proposed as a more sustainable alternative to LIBs.⁴⁻⁷

Xu and Angell discovered that lithium bis(oxalato)borate (LiBOB) could be considered as a fluorine-free salt alternative to the “standard” electrolyte salt of LiPF₆ for LIBs.⁸ One could therefore imagine the sodium counterpart, sodium bis(oxalato)borate (NaBOB), could be used for SIBs. As NaBOB, contrary to LiBOB, is not soluble in most commonly used non-aqueous solvents like carbonates, its application in SIBs was long neglected. Although its synthesis was previously already demonstrated by Zavalij in 2003,⁹ NaBOB was never used for SIBs until 2020, when we showed that NaBOB has a practical level of solubility in NMP as well as in flame-retarding alkyl phosphates such as trimethyl phosphate (TMP), providing promising ionic conductivities and electrochemical cycling.^{10,11} It has also been shown that Triethyl phosphate (TEP) can dissolve NaBOB up to 0.37 mol kg⁻¹ to provide an ionic conductivity of 5 mS cm⁻¹.¹² The reduction of the BOB⁻ anion in the first charge contributes to formation of the solid electrolyte interphase (SEI). For LIBs, LiBOB has shown to suffer from formation of too resistive SEI.⁷ For SIBs however, the use of

BOB⁻ anion could be beneficial to address the high solubility of SEI which is an issue in carbonate-based electrolytes in SIB.^{13,14}

Colbin et al.¹² has previously shown promising results on electrochemical cycling of SIB full-cells using NaBOB-TEP. However, a relatively low mass loadings of about 2 mg cm⁻² for positive and negative electrodes were used in the previous study. This study therefore aims to optimize NaBOB-TEP electrolyte using combinations of common SEI forming additives for full-cells with industrial mass loadings (>10 mg cm⁻²) and electrolyte volumes (<5 ml g⁻¹). The studied additives are chosen from a selection of chemicals successfully used in state-of-the-art carbonate electrolytes for LIBs, where the best results were found for electrolytes that combined additives from three distinctive groups of primary, secondary and tertiary additives in low concentrations.^{15,16} Fluoroethylene carbonate (FEC) is also chosen as an additive candidate due to its common use in SIB electrolytes. It should be noted that SEI-forming electrolyte additives is only one of many ways to improve cycling life of batteries. With a well-designed formation cycling protocol where cell voltage, temperature and c-rates are carefully controlled, high long-term cycling performance can in theory also be achieved.¹⁷

In this study, a series of electrolytes are studied employing combinations of the additives fluoroethylene carbonate (FEC), vinylene carbonate (VC), prop-1-ene-1,3-sultone (PES), 1,3,2-dioxathiolane 2,2-dioxide (DTD) and tris(trimethylsilyl)phosphite (TTSPi) in hard carbon—Prussian white full-cells (Fig. S1). Galvanostatic cycling of 2- and 3 electrode cells is used to determine the initial and long-term cycling performance of the electrolytes, and Coulombic efficiencies as well as cell polarization are compared among cells. Results from variety of characterization techniques including X-ray photoelectron spectroscopy and gas pressure analysis shed light on the reactions occurring at the electrode-electrolyte interfaces during cell cycling.

Experimental

Chemicals and materials.—NaBOB salt was synthesized according to the method by Zavalij⁹ and further purified according to the method described by Mogensen et al. in Ref. 11. FEC, DTD and

^zE-mail: reza.younesi@kemi.uu.se

TTSPi (from Aldrich), VC (from Gotion) and PES (from Sigma-Aldrich) were used as the electrolyte additives. Aluminum current collector tabs were used for both electrodes and a polyaramid based separator (Dreamweaver gold) cut to 30*30 mm squares and dried at 140 °C in vacuum.

Electrode foils were provided by LiFeSiZE AB. Cathodes consisted of 93 wt% ($\sim 12 \text{ mg cm}^{-2}$) Fennac® (commercial Prussian white cathode material powder) supplied by Altris AB, 4 wt% C65 carbon black additive (Imerys) and 3 wt% binder mixture (equal amounts of sodium carboxymethyl cellulose (NaCMC) and styrene butadiene rubber, (SBR)) slurry coated on aluminium foil, whereas anodes consisted of 96 wt% hard carbon (Kuranode type II) and 4 wt% of the same binder mixture. The mass loadings were balanced with a N/P ratio within 1.1–1.3, assuming a capacity of 150 mAh g^{-1} in Prussian white and 285 mAh g^{-1} in hard carbon. Electrodes were punched from foil sheets to 20 mm diameter circles and dried in a Büchi vacuum oven at 140 °C overnight and then stored in an argon filled glovebox ($P_{\text{H}_2\text{O}}$ and $P_{\text{O}_2} < 1 \text{ ppm}$) until assembled into battery cells.

Electrolyte preparation.—TEP solvent (Acros) was dried using molecular sieves in a glovebox, while NaBOB was thoroughly dried in a vacuum oven at 100 °C for over 12 h. From these components a 0.35 M stock solution was prepared by dissolving 6.6 wt% NaBOB in TEP, which constituted the limit of solubility.

All electrolytes with additives had a 3 wt% additive content, i.e. electrolytes with two additives had 1.5 wt% of each additive and electrolytes with three additives had 1 wt% of each additive. An overview of all used electrolytes is can be found in Table 1. The following is a description over how the electrolytes with 3 wt% of one additive was prepared inside a glovebox. To five 7 ml vials, one for each electrolyte additive, 6 ml of stock solution was added and weighed. For additives in liquid form, namely FEC, VC and TTSPi, the needed volumes were calculated using density values from literature. Half of the needed volume was added using a micropipette and the vial was weighed. The second half of additive amount was slightly recalculated reflecting the density of the first half. For the other additives, which were solid under room temperature conditions, needed amounts were weighed on an analytical balance with 0.1 mg precision. All electrolytes were clear after 10 s of violent shaking. The electrolyte that contained 3% DTD underwent a color change to pale yellow within two months and this electrolyte had to be re-made.

Galvanostatic cycling.—For each electrolyte composition, at least two pouch full-cells were cycled, and for some compositions also a 3-electrode cell. The electrolyte volume in each cell was equal to 150 μl . The cells were taken out of the glovebox and put under stack pressure between 3 mm plastic plates and clamped before galvanostatic cycling at room temperature in either of the equipment

Table I. A list over the prepared electrolytes. All electrolytes were based on 0.35 M NaBOB in TEP, except the two based on 1 M NaPF₆ in 1:1 EC:DEC. In electrolytes with additives, the total additive content is 3%.

One additive	Two additives	Three additives
FEC	FEC+VC	FEC+VC+PES
VC	FEC+PES	FEC+VC+DTD
PES	FEC+DTD	FEC+VC+TTSPi
DTD	FEC+TTSPi	FEC+PES+DTD
TTSPi	VC+PES	FEC+PES+TTSPi
NaBOB–TEP-ref	VC+DTD	FEC+DTD+TTSPi
EC:DEC-ref	VC+TTSPi	VC+PES+DTD
EC:DEC+5%FEC-ref	PES+DTD	VC+PES+TTSPi
	PES+TTSPi	VC+DTD+TTSPi
	DTD+TTSPi	PES+DTD+TTSPi

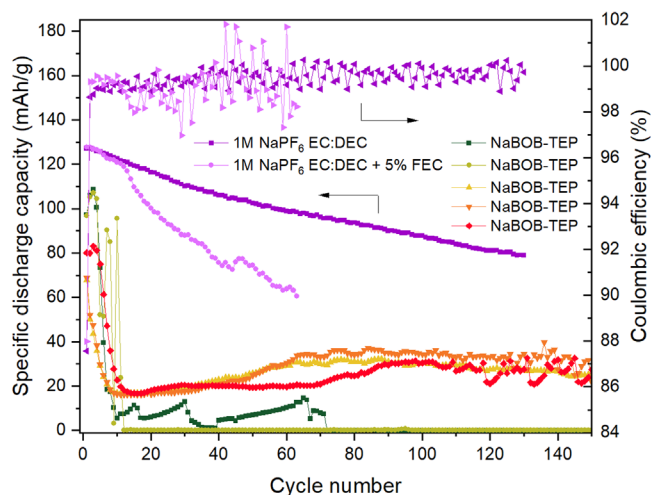


Figure 1. Reference cells using either 0.35 M NaBOB in TEP electrolyte without additive ("TEP-ref") or 1 M NaPF₆ in EC:DEC 1:1, with or without 5 wt% FEC additive in full-cell SIBs with high mass loading Prussian white and hard carbon electrodes. Capacity values are specific in relation to the cathodes active mass.

LAND CT2001A battery tester or Neware BTS4000 galvanostat after a 12 h rest period. C-rates were calculated assuming a capacity of 150 mAh g^{-1} in the PW cathode. The cycling was generally performed using 0.2 C rate. 3-electrode cells were cycled for 10 cycles in a Biologic MPG-2 potentiostat at 0.1 C rate. The upper and lower cut-off potentials were 3.8 V and 1.3 V, respectively. 3-electrode cells used reference electrodes consisting of Prussian white partly desodiated to the middle of the upper voltage plateau at around 3.3 V vs Na⁺/Na, in accordance with the procedure described in Ref. 11. All cell assembly was performed in an argon filled glovebox.

XPS.—Hard carbon electrodes were cycled for one full cycle at 0.2 C after a 48 h rest period. One electrode was soaked in the additive-free NaBOB–TEP electrolyte for 48 h and one pristine electrode was also used. After cell disassembly, all electrodes including the soaked and pristine electrodes were cut to smaller pieces, then washed with pure TEP and dried in a vacuum oven overnight in room temperature. The electrode pieces were placed on an insulating sample plate and analyzed in a Kratos AXIS Supra +tool using the photon excitation energy of 1487 eV (Al K α). The binding energies in the recorded XPS spectra were calibrated so that the sp² C=C peak of hard carbon was placed at 284 eV for pristine and soaked samples and the sp³ C–C peak was placed at 285 eV for cycled samples. All sample preparation was made in argon atmosphere within a glovebox to protect the electrodes from air, and the samples were transferred to the XPS analysis chamber using a sample holder with an airtight lid.

Pressure analysis.—The pressure monitoring was performed in a helium-leak tested pressure cell (PAT-Cell-Press) of El-Cell® GmbH, Germany. The PAT-Cell-Press consists of a lower plunger, upper plunger and insulation sleeve which were all used as-delivered by El-Cell. The plungers are made of aluminum, acting as current collectors. The insulation sleeve contains a pre-dried 260 μm borosilicate-glass fiber separator which has a diameter of 18 mm (GF/A of Whatman®, United Kingdom). All electrodes were punched to a diameter of 18 mm and dried according to the earlier described drying process. The cell setup is helium leak tested and guaranteed a minimum leakage rate of 0.3 mbar h⁻¹. A schematic overview of this cell is shown in Fig. S15. The cells were assembled with 100 μl electrolyte in an argon-filled glovebox. After assembly the cells were placed in a climate chamber (KB53, Binder® GmbH) and cycled at 30 °C using a Biologic potentiostat at 0.2 C for 3

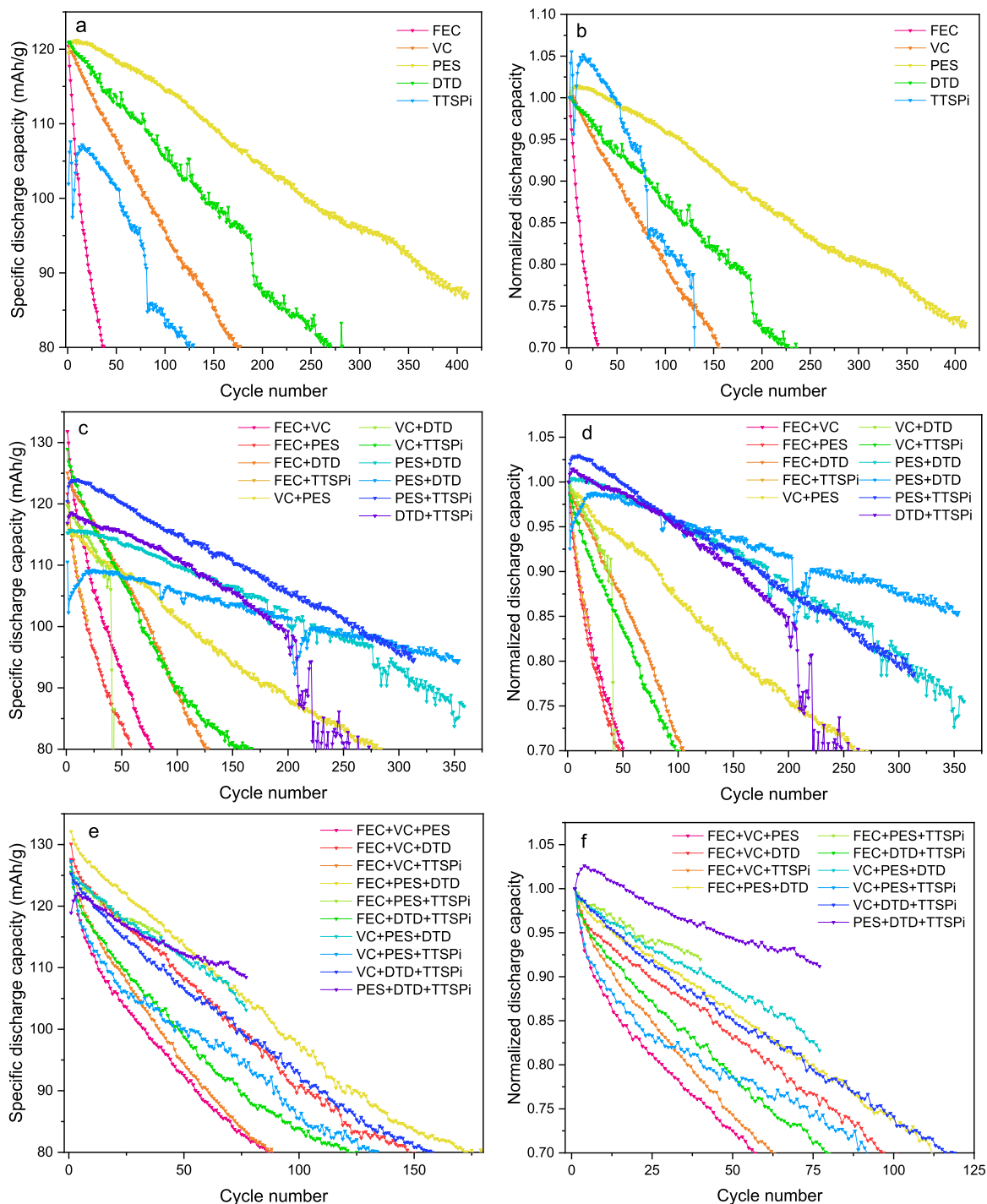


Figure 2. Specific discharge capacities (relative to cathode active mass) of sodium-ion full-cells containing 0.35 M NaBOB–TEP with electrolyte additives cycled at 0.2 C. In (a) and (b) one additive, (c) and (d) two additives and (e) and (f) three additives were used. The cell name reflects the content of electrolyte additives in each electrolyte with a total additive content of 3 percent by weight with equal weighting to each additive.

cycles, between 3.8 V and 1.3 V cut-off potentials. Gas leakage out of the cell is specified at maximum 0.3 mbar h^{-1} .

Results and Discussion

Five different electrolyte additives in single, binary, or ternary mixtures were added to NaBOB–TEP electrolyte solution to investigate electrochemical performance of SIB full-cells with high mass loading Prussian white and hard carbon electrodes. A few different reference electrolytes such as NaBOB–TEP without

additive and EC:DEC based electrolytes were also used for comparison with the electrolytes with additives.

Galvanostatic cycling performance.—Figure 1 shows electrochemical cycling of five identical reference cells with 0.35 M NaBOB in TEP electrolyte without any additives at 0.2 C rate. Two reference cells with carbonate based electrolytes of 1 M NaPF₆ in 1:1 EC:DEC electrolyte were also cycled, one of them with 5% FEC as an additive. All the five NaBOB–TEP reference cells showed very fast decline in discharge capacities within the first 10 cycles.

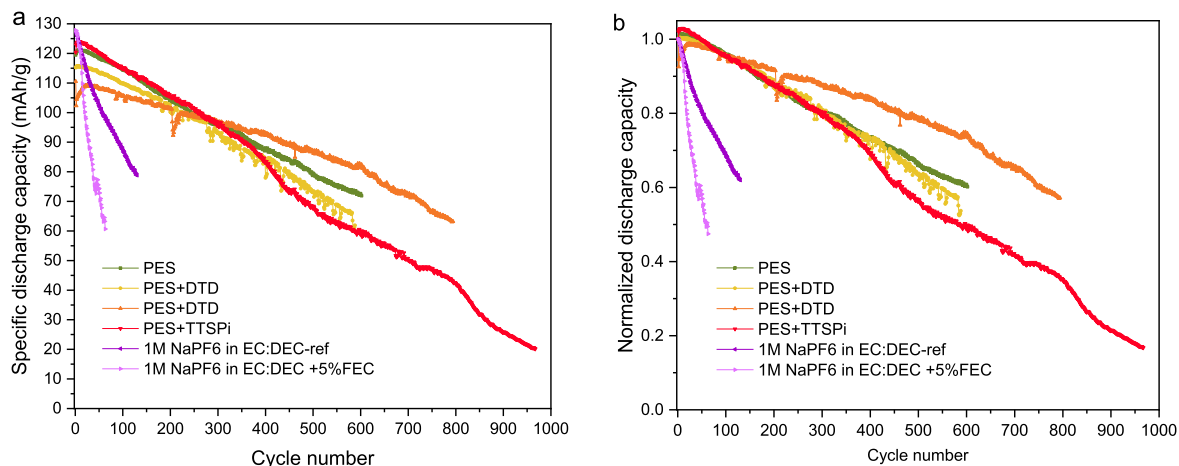


Figure 3. (a) Specific discharge capacities relative to cathode active mass and (b) normalized capacities for a selection of champion cells with electrolytes based on 0.35 M NaBOB in TEP as well as reference cells using a standard 1 M NaPF₆ in 1:1 EC:DEC electrolyte, with or without 5% FEC addition. The cell name reflects the content of electrolyte additives in each electrolyte. The two cells marked with PES+DTD are duplicate cells with the same electrolyte. A wider selection of best cells can be found in Fig. S9.

The cycling performance is inferior compared to the previous work in which much lower mass loading were used; that is $\sim 2 \text{ mg cm}^{-2}$ in previous study compared to $\sim 12 \text{ mg cm}^{-2}$ here.¹² It is reasonable to assume that the SEI-formation is affected by the high anode mass loading and high applied current in initial cycles, which indicates that the reference NaBOB–TEP electrolyte cannot form an efficient SEI in such condition. Post-mortem analysis of three of the five cells reveals no delamination of electrode material from current collectors on either the anode or the cathode.

In Figs. 2 and 3, which show the best cell of each additive combination, all the tested additives are shown to be effective, to different extent, at enhancing the electrochemical cycling performance, at least compared to the reference cells in Fig. 1. The PES additive shows most promising results with and without adding DTD and/or TTSPi, as it is evident in Fig. 3. Cells using these electrolytes tend to increase in discharge capacity for the first 5 cycles. The capacity retention in long-term cycling is markedly larger than for both reference electrolytes (NaBOB–TEP and EC:DEC). Combinations incorporating FEC

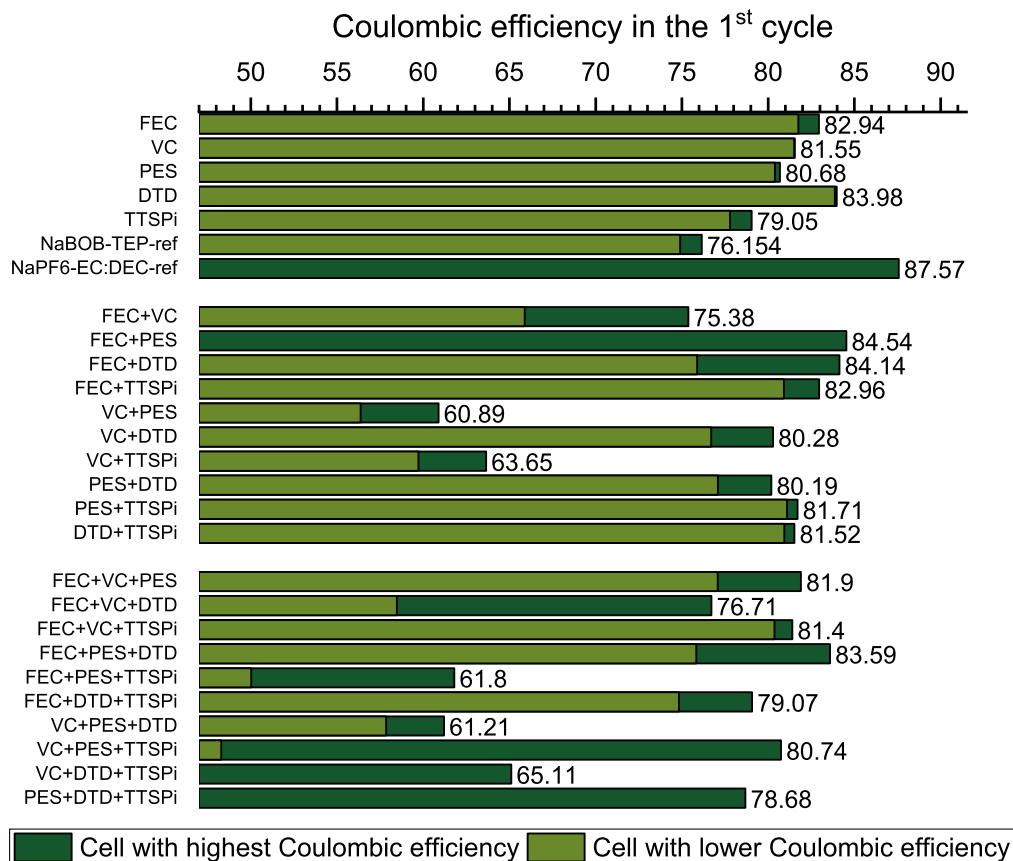


Figure 4. 1st cycle Coulombic efficiency for the cells using electrolytes with one, two or three additives as well as the reference cells using NaBOB–TEP or 1 M NaPF₆ in 1:1 EC:DEC. The label numbers are for the best ICE of each electrolyte.

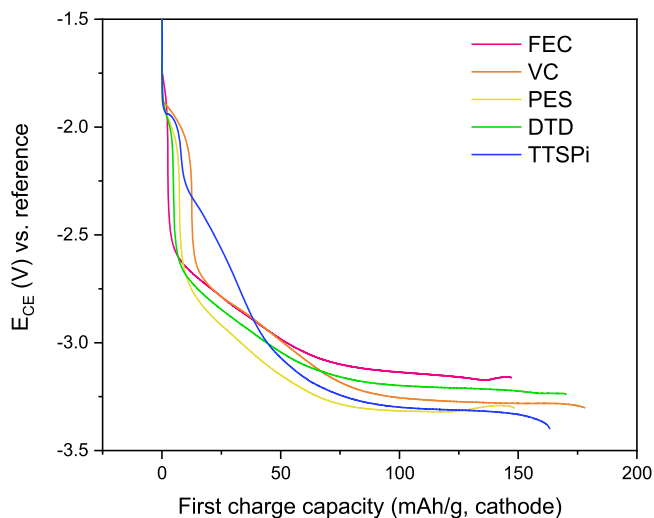


Figure 5. Voltage of the hard carbon counter electrode (anode) vs a partly desodiated Prussian white reference electrode during the first cycle charge (0.1 C), when the SEI initially deposits.

generally shows good initial Coulombic efficiency, but suffer from a rapid and steady capacity fading as cycling progresses. After the first few cycles, most of the cells have a relatively linear decline in discharge capacity, except for cells containing FEC, which initially show a rapid capacity fade which subsides slightly, although the cells with FEC+DTD seem to adhere to the linear decline (see Fig. 2). Extended cycling performance of all cycled cells is further presented in Figs. S2–S4. The first prepared electrolyte with DTD showed poor cycling performance in cells and since a color change was observed in this electrolyte after storage, cells were remade with fresh electrolyte (see comparison in Fig. S5).

Initial coulombic efficiency (ICE).—Figure 4 displays the ICE values -referring to the Coulombic efficiency of the 1st cycle—for two identical cells of each electrolyte solution; the cell with

higher ICE is shown by dark green with the exact ICE value written, and the cell with lower ICE is displayed with light green. The ICE values give clues about the effectiveness of SEI formation. No electrolyte matches the high ICE value of the EC: DEC reference, although some—especially DTD—come close. All single additive cells perform better than the TEP reference cells except TTSPi and one cell with DTD. It should be noted that although ICE values for cells containing FEC were relatively high, the long-term cycling quickly erodes the discharge capacity, as can be seen in Fig. 2.

Voltage profiles.—Apart from two-electrode full-cells, three-electrode cells were also cycled using partially desodiated Prussian white as a reference electrode in order to elucidate the voltage profile of the hard-carbon (Figs. S7–S12 and Fig. 5). The voltage curves show the distinct reduction plateau seen at around 1.6–1.9 V for a NaBOB-containing electrolyte, indicating that the BOB[−] anion takes part in the SEI formation. The width of the plateau should correlate with the degree to which BOB[−] is used. Some additives, especially FEC, have a narrower plateau, which indicates that the additive decreases the role of NaBOB in SEI formation. The plateau size in the first cycle, starting at around −1.9 V (vs the partially desodiated Prussian white reference electrode) and measured in mAh g^{−1}, can from Fig. 5 be described as FEC < DTD < PES < TTSPi < VC. Note that TTSPi has a large sloping feature after the plateau indicating that the decomposition of TTSPi continues at lower potentials, which can also be seen for the DTD+TTSPi cell (Fig. S12). The small role of SEI related to BOB- products may be the reason for the poor long-term cycling performance of cells with electrolytes containing FEC.

Interestingly, the anode voltage for FEC and PES goes up towards the end of the first charge (Fig. 5), which most likely is due to sodium plating on the anode. Especially on the FEC-curve, where the voltage has a clearly visible bounce. This is an indication that either the positive to negative active material mass ratio in these cells were not properly balanced or the cell resistance led to sodium plating.

Many cells experience problems reaching the higher cut-off potential of 3.8 V during charge, indicating side-reactions on the anode, most probably electrolyte decomposition. A review of

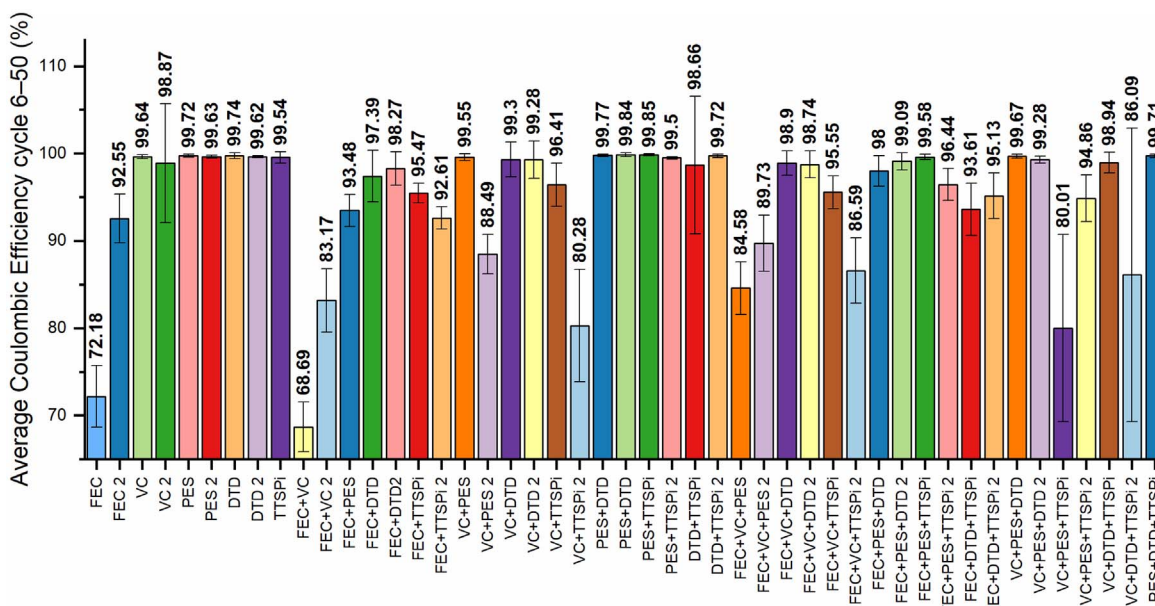


Figure 6. Average Coulombic efficiencies (values in the numerical labels) in cycles 6–50 for most cells. Black lines are error bars showing the standard deviation. Cell names without numbers are the same cells that are shown in Fig. 2 whereas cell names marked with the number 2 are duplicate cells with lower capacity retention in long-term cycling.

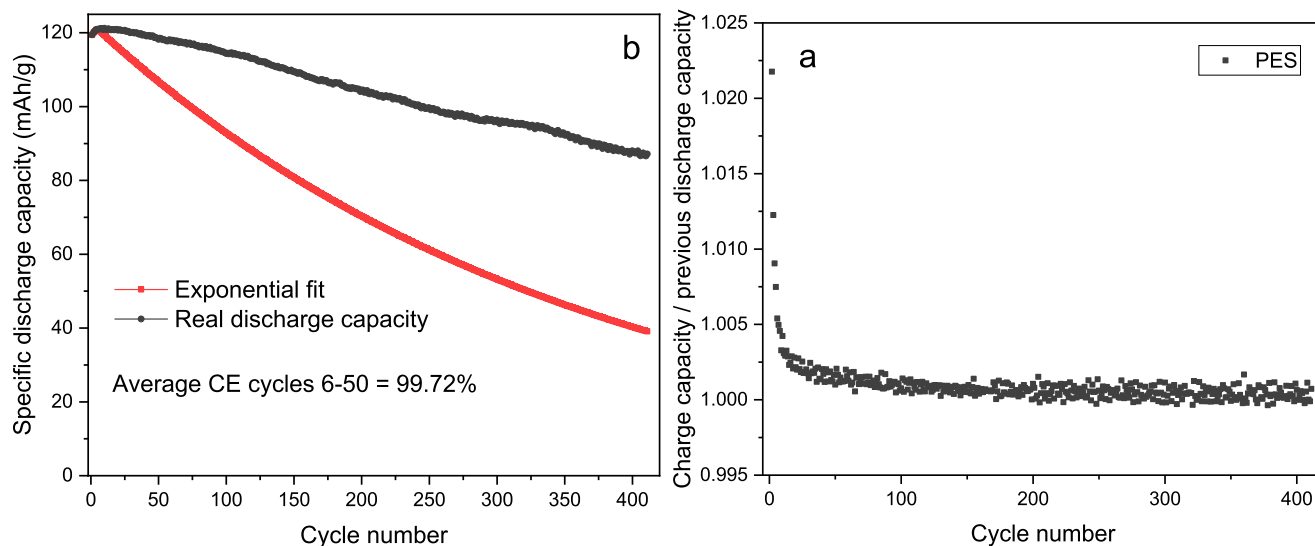


Figure 7. (a) The average Coulombic efficiency of cycle 6–50 was used to construct a theoretical curve of exponential specific discharge capacity degradation (red) for the top performing PES cell, after the 5 first cycles. Capacity values are specific in relation to the cathodes active mass. (b) Plot of charge capacity divided by the discharge capacity of the previous cycle for the top performing PES cell.

voltage curves for all the cells shows that almost all electrolytes using FEC have at least 1 cell out of 2 with severe side-reactions from the first cycle and onwards. The exceptions were FEC+PES and FEC+PES+DTD for which the side-reactions appear for later cycles but not the first cycle. Most electrolytes with VC also suffer severely from side-reactions, except for VC and VC+DTD. No electrolyte without FEC and VC suffer severely from side-reactions. These results mirror the measured CE values for the first cycle, where side-reactions and low CE values correlate (Fig. 4).

Comparison of polarization and CE after formation.—Coulombic efficiency and polarization were measured to further evaluate the cycling performance. The average values of CE after the first five cycles (i.e. cycles 6 to 50) are displayed in Fig. 6. From these results, we assume that the SEI had formed “completely” formed during the first five cycles, and therefore CE below 100% indicates other irreversible reactions originated. Although some cells experience severe side-reactions, as is manifested in low Coulombic efficiency values, both for the first cycle and often also for consecutive cycles, the discharge capacity is often maintained fairly well. One clear example of this, out of many, is the VC+PES combination, which is used in two cells with similar capacity retention performance (Fig. S3). Cell 1 has a high average CE of 99.55% whereas cell 2 has only 88.49%. Another example is the 3% PES electrolyte which provides top performing cells, but based on average CE values after SEI formation (cycles 6–50), the capacity should theoretically degrade faster, based on the theoretical assumption that a low CE equals consumption of sodium capacity (Fig. 7a). To have a better understanding on this, the charge capacity of each cycle divided by the discharge capacity of the previous cycle is plotted in Fig. 7b. The values shall in theory be maximum equal to one, but the results show values higher than one. This implies that some sodium reservoir is available in the cathode which is slowly extracted over cycling. For cells using electrolytes with FEC or VC, that often have very high charge capacities, this phenomenon is even clearer, with some interesting trends (Fig. S13).

To analyze the polarization present in cells, voltage curves were studied numerically to calculate the voltage difference at 40 mAh g⁻¹ from the start of the charge and discharge of a certain

cycle, respectively. An example of this is shown in Fig. 8. Polarization values in cycle 2, 10 and 50 are then summarized in Fig. 9 for a selection of best cells. Only cycle 2 was calculated for the TEP-reference cells, as their discharge capacities quickly degrade below 40 mAh g⁻¹ within 10 cycles. Polarization correlates with the real anode DC resistance but also contains the IR drop of the electrolyte. Polarization calculations can hence be viewed as a quick alternative to impedance measurements although there are many contributions included in the total resistance.

Since polarization leads to lower energy efficiency by means of a lower discharge voltage and also limits the cell from using the full inventory of sodium capacity, leading to capacity degradation, it should ideally be low and not increase. When beneficial additive combinations are used, the polarization is lower in cycle 2 than the TEP-ref cells, as can be seen in Fig. 9. Some exceptions can be seen for cells that drops in capacity the first cycles and recover in later cycles (e.g. PES+DTD 2). It is also clear that additives that helps long-term cycling performance, such as PES, PES+DTD and DTD+TTSPi also give favorably low polarization values that also decrease with cycling. In contrast, cells with less favorable additive combinations such as those that contain FEC, do not see the same reduction of polarization in later cycles. Furthermore, we can see that between the cells with the same electrolyte, the cell with the best capacity retention often has a lower polarization in all cycles than the other cell (cells marked with the number 2 in Fig. 9). It should be noted that the higher polarization in the first cycles compared to later cycles for the best cells is a result of SEI formation and is unavoidable.

X-ray photoelectron spectroscopy (XPS).—To investigate the composition of the SEI, samples from hard carbon anodes cycled one full cycle in full-cells with five selected electrolyte compositions were examined further using X-ray photoelectron spectroscopy, along with a pristine anode and an anode soaked in the additive-free electrolyte. So, hard carbon anodes from cells with NaBOB–TEP without additives, and with PES, PES+DTD, PES+TTSPi and PES+DTD+FEC were analyzed (see Fig. 10).

The XPS spectra in Fig. 10 indicate that the variation in electrolyte choice has some consequences on the composition of

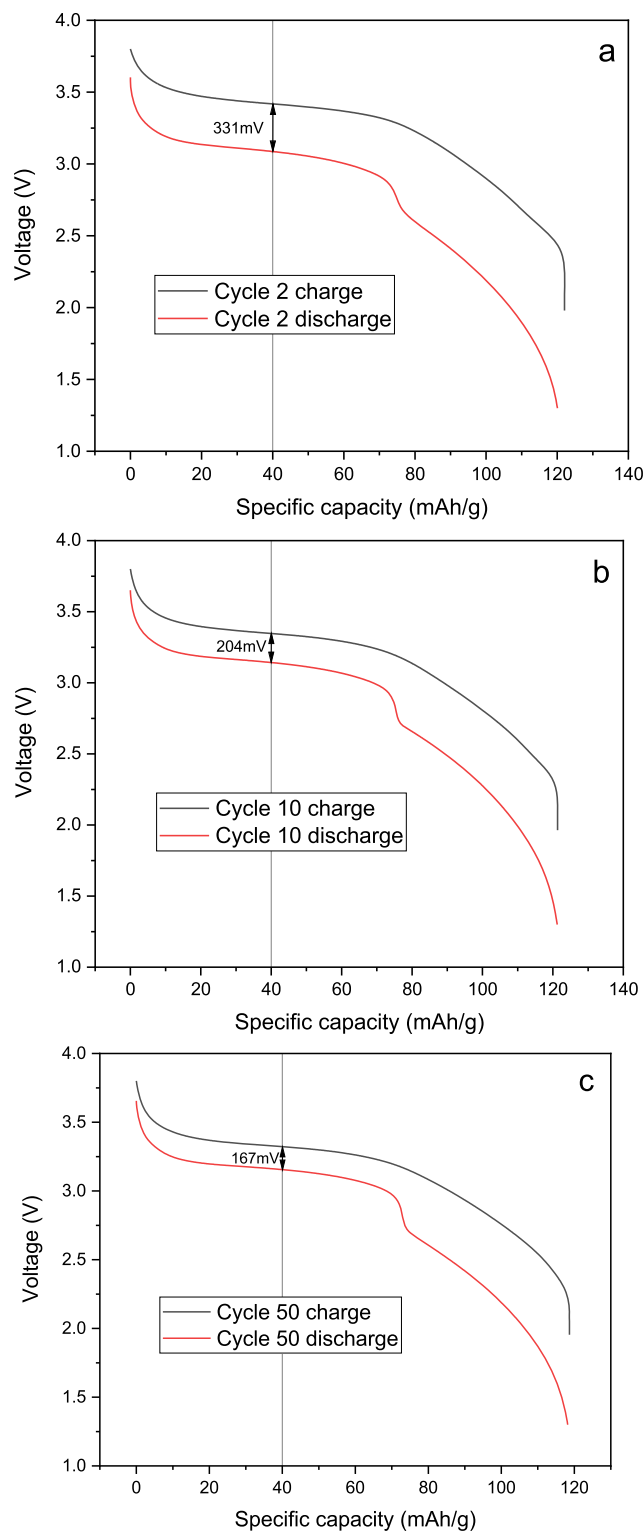


Figure 8. Visualization of the polarization of the top performing PES cell in cycle 2 (top), cycle 10 (middle) and cycle 50 (bottom). Capacity values are specific in relation to the cathodes active mass.

SEI on hard carbon electrodes. In the C 1s spectra, the pristine and soaked electrodes show a main peak calibrated to 284.0 eV that represents the sp^2 hybridized carbon ($C=C$) in the hard carbon active material. Some peaks at higher binding energy in the spectrum of the pristine sample represent other carbon species in the binders, as is noted in the figure. In the cycled electrodes, the peak representing

$C=C$ is shifted to a lower binding energy of 282.7 eV. This can be explained either by residues of sodiated hard carbon or by a buried interface (dipole layer) between the newly formed SEI and the bulk electrode.¹⁸ The peak height is diminished, confirming that the hard carbon is covered by SEI, and that the thickness of the SEI is thinner than probing depth. It is clear that cycled samples contain $O-C=O$

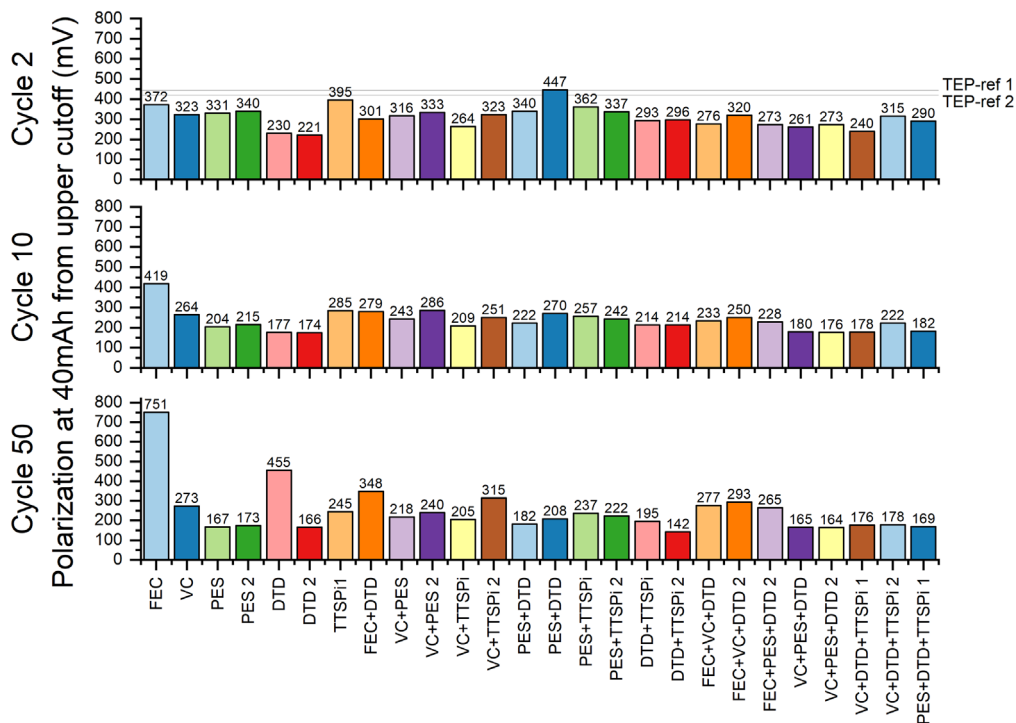


Figure 9. Polarization for a selection of best cells in cycle 2, 10 and 50, noted as a voltage difference between the charge curve and the corresponding discharge curve, both at 40 mAh from the upper cutoff. Values for the two best NABOB–TEP reference cells at 420 and 443 mV in cycle 2 is shown as horizontal lines. The cell names without numbers are the same cells that are shown in Fig. 2 whereas cell names marked with the number 2 are duplicate cells with lower cycling performance. Outlier values of FEC and DTD cells in cycle 50 are related to anomalous voltage profiles, of which one example is shown in Fig. S14.

species, which corresponds to an SEI derived from ring-opening of BOB⁻ anions, producing oxalate (O–CO–CO–O) and/or esters alkyl carbonate (ROCOONa) species (semicarbonates), which has been proposed in literature for electrolytes containing LiBOB,^{19–22} or possibly branched poly(BOCOO).¹⁹ This peak was already present in the NaCMC binder in the pristine sample, but it is likely shielded by the SEI. In C 1s spectra, very small differences are observed between the cycled samples including the sample without additives, which however has a more pronounced C=O peak. The highest peak in the cycled samples is assigned to hydrocarbon species. The C–O peak from the binder at 286.6 in the pristine and soaked electrodes is still present after cycling, which could indicate formation of ether species in the SEI, possibly PEO (–CH₂–CH₂–O–), which is in agreement with literature, although the concentration (peak area) is usually lower compared to the semi carbonates peak.^{19–22}

In the B 1s spectra, the “no additive” sample displays a larger contribution from the peak at 192.6 eV assigned to B–O_x (x = 3 or 2) species, suggesting that decomposition of NaBOB plays a larger role in the SEI formation compared to the cells with additives. This is in line with the discussion in relation to Fig. 5. Peaks assigned to Cl 2p species (Cl 2p_{3/2} and Cl 2p_{1/2}) are present in the pristine electrode as well as in all cycled electrodes. The source of this chlorine could be NaCl impurities in the binder, that shows up as metal chlorides in the pristine anode but is dissolved from the surface of the soaked electrode. One other, more probable, theory is that the paper sheets put between electrodes in the drying step contains chlorine compounds used in pulp bleaching, that diffuse into the surface of the electrodes. Both peaks in the O 1s spectra are strengthened in cycled samples which is consistent with the finds in the C 1s spectra.

In the P 2p spectra, characteristic peaks at 133.6 eV and 134.3 eV are recognized, representing P–O and phosphate species, respectively. The soaked sample has some of both species, indicating some residues of TEP from the soaking. Interestingly, for all cycled electrodes except for the PES sample, the peaks for both species are

large, with a preference towards P–O for the TTSPi-containing sample, stemming from the P–O present in the TTSPi molecule, and for the “no additive” sample, whereas phosphates are preferred in the PES+DTD and PES+DTD+FEC samples. The low peaks in the PES sample could indicate that PES is preferentially consumed in the SEI formation for this electrolyte recipe. The higher P–O peak in the additive-free sample indicates that a higher share of the SEI is derived from TEP.

A small contribution from metal fluorides (NaF) and organic C–F can be found in the F 1s spectra for all cycled anodes, although they are much larger in the fluorine containing PES+DTD+FEC electrolyte. These artefacts are possibly due to contaminations in the drying step, since fluorine is not expected on the other cycled samples. The peaks at 1071.5 eV in the Na 1s spectra for all the five cycled anodes is an evidence of Na species in the SEI. The low peak in the pristine sample originates from the Na⁺ present in the NaCMC binder.

Species containing both –SO₃ (at 166.0 eV) and other SEI species, possibly –SO₄ (S 2p_{3/2} at 168.0 eV and S 2p_{1/2} at 169.1 eV) in the S 2p spectra are found to correlate in peak intensity with the content of PES additive in the specific electrolyte, which is evidence that these species are derived from PES. –SO₄ based species (S 2p_{3/2} at ~168.7 eV and S 2p_{1/2} at 169.9 eV) were also detected for the samples containing DTD. This can be explained by the SO₃²⁻ and SO₄²⁻ environments present in the PES and DTD molecules, respectively, and it differs from interpretations found in literature on PES for graphite electrodes.²³ For the pristine and soaked electrodes, as well as the “no additive” electrode, no signal was recorded, as expected.

The responses in the Si 2p region show Si–O_x characteristics which is strongest for the Si-containing DTD+TTSPi electrolyte, where TTSPi is a source of Si. The detected Si in the other samples was likely originated from the paper sheets put between electrodes since no Si should be present there.

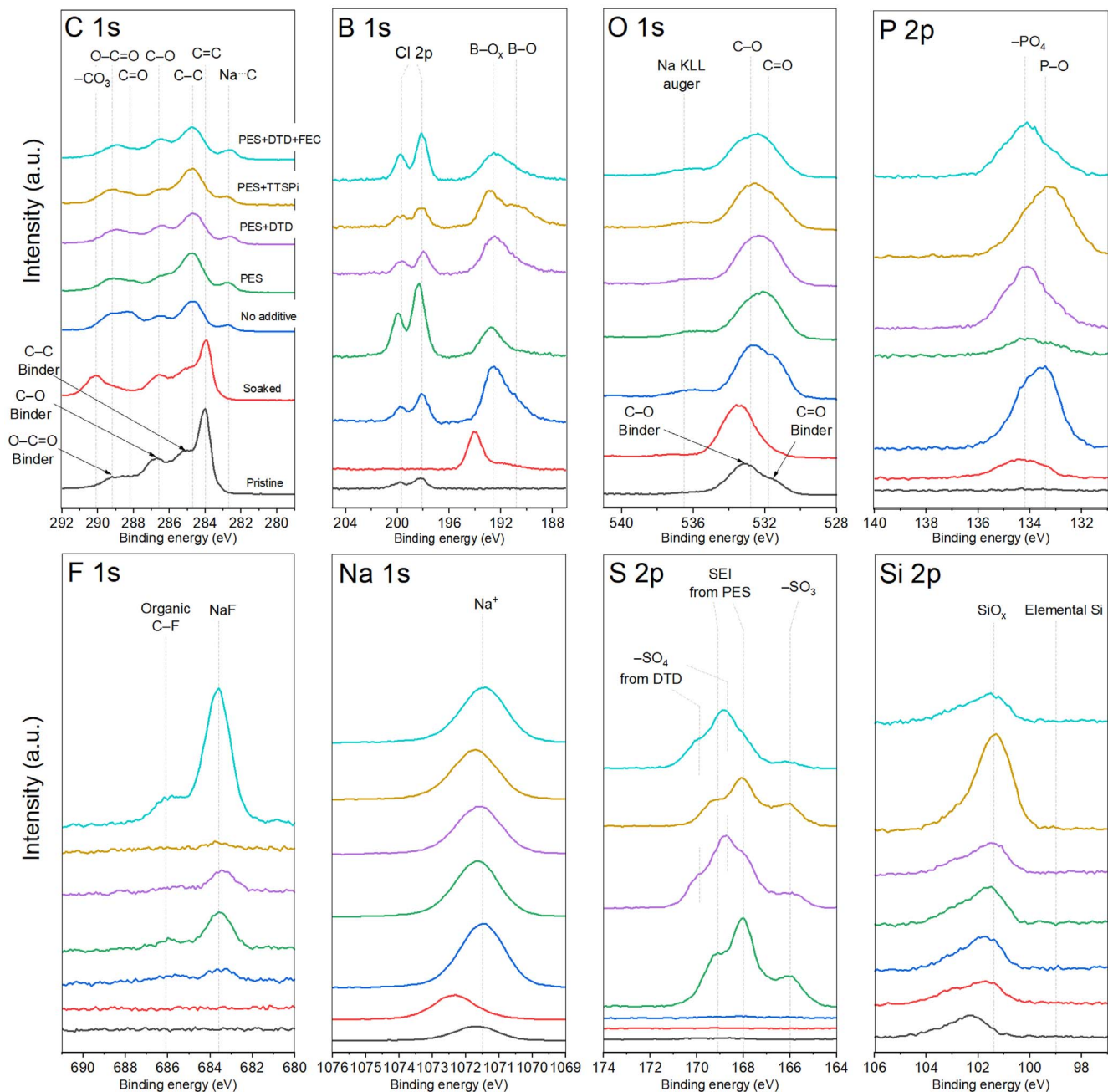


Figure 10. XPS spectra for hard carbon electrodes cycled one cycle in full-cells against Prussian white cathodes using 5 different electrolyte compositions based on NaBOB–TEP of which four incorporated an electrolyte additive (see legend), along with a pristine anode and an anode soaked 2 days in the additive-free electrolyte. The spectra are not normalized.

Pressure analysis.—To gain better understanding about the electrolyte stability, pressure measurements were performed during 3 formation cycles on full cells using the same electrolytes as were studied with XPS. The increase in pressure was assumed to be solely from gas formation in the cell. Figure 11 shows that a minimal gas was formed from all the electrolytes, except for PES+DTD+FEC where a significant gas pressure increase was recorded. This electrolyte gives the highest initial coulombic efficiency of 85.10% among the cells cycled for pressure analysis, which is consistent with the other results. It has previously been shown that FEC decomposes with gaseous products such as ethylene, carbon dioxide and carbon monoxide during SEI formation.^{24,25} Here, it is evidence that FEC actively takes part in the SEI formation, leading to high initial coulombic efficiency, but as previously mentioned, the cells

with FEC also suffer from higher long-term capacity degradation which may be related to the gaseous products.

For the other cells, mainly solid decomposition products are thus formed. PES shows an effect of lowering the amount of gas formation, relative to the electrolyte without additives. Noticeably, the addition of TTSPi to the electrolyte containing PES further reduces the pressure, whereas the presence of DTD invokes a slight increase in pressure.

Conclusions

Sodium-ion cells with high-mass loading electrodes ($\sim 12 \text{ mg cm}^{-2}$) cycled at 0.2 C rate suffers from poor cycling performance when NaBOB–TEP electrolyte without additives was used. These

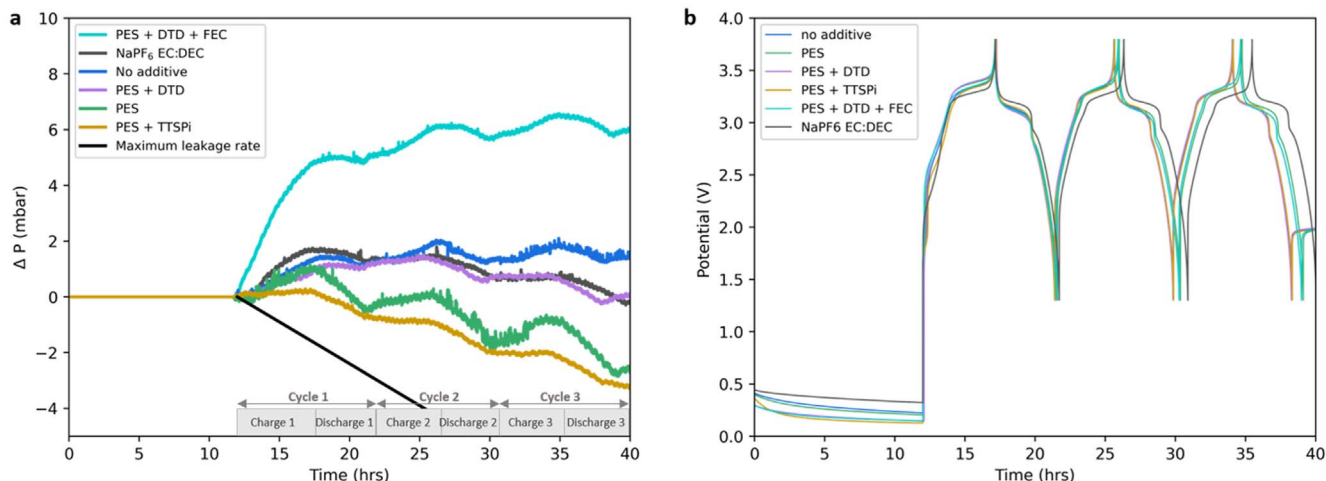


Figure 11. (a) Pressure analysis of full-cells containing NaBOB–TEP electrolytes with different additive combinations as well as reference cells with additive-free NaBOB–TEP and 1 M NaPF₆ in EC:DEC 1:1, respectively. Total additive content is 3 wt%. Note that an extra graph is added to show the maximum pressure decrease due to cell leakage. (b) Voltage profiles of the same cells during the pressure analysis test.

cells fall to low or zero discharge capacity within the first 12 cycles, although, a carefully designed formation cycling at lower C-rates (or, as recently have been discovered in unpublished results, elevated temperature) would certainly be beneficial. The chosen cycling method cause the electrolyte properties to be highlighted, rather than hidden.

Some additives greatly enhanced both the Coulombic efficiency and discharge capacities as compared to reference cells using NaBOB–TEP electrolyte without additives. Both the electrode mass loadings and electrolyte volumes are close to the what is used in commercial cells, and considering that no formation cycling was performed on cells in this study, the results are impressive. This is a screening experiment to map the system and thus does not include important factors such as formation protocol, additive amount optimizations etc. The best performing electrolyte compositions in this study are still not good enough for commercial use, but shows that non-flammable fluorine-free electrolytes can be used with high-mass loading electrodes in full cell sodium-ion batteries using hard carbon and Prussian white. Further optimization is needed to enhance the long-term cycling performance and initial Coulombic efficiency. In any case, going to higher rate than 0.2 C, which is desired for commercial use, might be too much for the ionic conductivity of 5 mS cm^{-1} obtained for 0.4 M NaBOB in TEP = $0.37 \text{ mol kg}^{-1,12}$ at room temperature, and thus might require the use of co-solvents.

PES and/or DTD, with or without TTSPi seems to work well in forming an SEI that is stable for long-term cycling, which is similar to what have been observed for lithium-ion batteries. It is interesting to see that unlike in LIBs, FEC and VC does not help with the formation of a long-term stable SEI, although the cells have initially high capacities. On the contrary, cells using electrolytes without FEC perform better long-term, although it is clear that cells with FEC and VC perform much better than the reference cells without any additives.

Further optimization of the additive concentrations in this electrolyte system might show even more stable cycling, and combined with a carefully designed formation cycling protocol possibly reaching a performance of commercial interest for sodium-ion batteries. Still, the limited ionic conductivity of the electrolyte may restrict the applications to lower C-rates.

Acknowledgments

The authors would like to acknowledge the financial contributions from the Swedish Energy Agency via project no. 50177–1 and via StandUp for Energy, from VINNOVA via BASE (Batteries

Sweden, no. 2019–00064), and from the EU project SIMBA (Sodium-Ion and Sodium Metal Batteries for Efficient and Sustainable Next-generation Energy Storage) a European Union H2020 research and innovation programme under Grant agreement No 963542.

ORCID

Reza Younesi  <https://orcid.org/0000-0003-2538-8104>

References

1. E. A. Olivetti, G. Ceder, G. G. Gaustad, and X. Fu, *Joule*, **1**, 229 (2017).
2. B. Ravdel, K. M. Abraham, R. Gitzendanner, J. DiCarlo, B. Lucht, and C. Campion, *J. Power Sources*, **119–121**, 805 (2003).
3. M. Zackrisson, L. Avellan, and J. Orlenius, *J. Clean. Prod.*, **18**, 1519 (2010).
4. Y. Huang, Y. Zheng, X. Li, F. Adams, W. Luo, Y. Huang, and L. Hu, *ACS Energy Lett.*, **3**, 1604 (2018).
5. C. Vaalma, D. Buchholz, M. Weil, and S. Passerini, *Nat. Rev. Mater.*, **3**, 18013 (2018).
6. R. Gond, W. van Ekeren, R. Mogensen, A. J. Naylor, and R. Younesi, *Mater. Horizons*, **8**, 2913 (2021).
7. G. Hernández, R. Mogensen, R. Younesi, and J. Mindemark, *Batter. Supercaps*, **5**, e202100373 (2022).
8. W. Xu and C. A. Angell, *Electrochim. Solid-State Lett.*, **4**, L3 (2001).
9. P. Y. Zavalij, S. Yang, and M. S. Whittingham, *Acta Crystallogr., Sect. B: Struct. Sci.*, **59**, 753 (2003).
10. R. Mogensen, S. Colbin, A. S. Menon, E. Björklund, and R. Younesi, *ACS Appl. Energy Mater.*, **3**, 4974 (2020).
11. R. Mogensen, A. Buckel, S. Colbin, and R. Younesi, *Chem. Mater.*, **33**, 1130 (2021).
12. L. O. S. Colbin, R. Mogensen, B. Alexander, Y.-L. Wang, A. J. Naylor, J. Kullgren, and R. Younesi, *Adv. Mater. Interfaces*, **8**, 2101135 (2021).
13. R. Mogensen, D. Brandell, and R. Younesi, *ACS Energy Lett.*, **1**, 1173 (2016).
14. L. A. Ma, A. J. Naylor, L. Nyholm, and R. Younesi, *Angew. Chemie Int. Ed.*, **60**, 4855 (2021).
15. L. Ma, J. Xia, and J. R. Dahn, *J. Electrochem. Soc.*, **162**, A1170 (2015).
16. D. Y. Wang et al., *J. Electrochem. Soc.*, **161**, A1818 (2014).
17. B. Kishore, L. Chen, C. E. J. Dancer, and E. Kendrick, *Chem. Commun.*, **56**, 12925 (2020).
18. J. Maibach, F. Lindgren, H. Eriksson, K. Edström, and M. Hahlin, *J. Phys. Chem. Lett.*, **7**, 1775 (2016).
19. K. Xu, U. Lee, S. Zhang, M. Wood, and T. R. Jow, *Electrochim. Solid-State Lett.*, **6**, A144 (2003).
20. A. Xiao, L. Yang, B. L. Lucht, S.-H. Kang, and D. P. Abraham, *J. Electrochem. Soc.*, **156**, A318 (2009).
21. S. Santee, A. Xiao, L. Yang, J. Gnanaraj, and B. L. Lucht, *J. Power Sources*, **194**, 1053 (2009).
22. Y. An, P. Zuo, X. Cheng, L. Liao, and G. Yin, *Electrochim. Acta*, **56**, 4841 (2011).
23. M. Li, B. Xu, Y. Li, L. Liu, W. Li Yang, and S. Hu, *Electrochim. Acta*, **105**, 1 (2013).
24. Y. Zhang, D. Krishnamurthy, and V. Viswanathan, *J. Electrochem. Soc.*, **167**, 70554 (2020).
25. A. L. Michan, B. S. Parimalam, M. Leskes, R. N. Kerber, T. Yoon, C. P. Grey, and B. L. Lucht, *Chem. Mater.*, **28**, 8149 (2016).